Genotype-Phenotype of Isolated Foveal Hypoplasia in a Large Cohort: Minor Iris Changes as an Indicator of *PAX6* Involvement

Yi Jiang, Shiqiang Li, Xueshan Xiao, Wenmin Sun, and Qingjiong Zhang

State Key Laboratory of Ophthalmology, Zhongshan Ophthalmic Center, Sun Yat-sen University, Guangzhou, China

Correspondence: Qingjiong Zhang, FARVO, Pediatric and Genetic Eye Clinic, Zhongshan Ophthalmic Center, Sun Yat-sen University, 54 Xianlie Road, Guangzhou 510060, China;
zhangqji@mail.sysu.edu.cn. or
zhangqingjiong@gzzoc.com.

Received: April 6, 2021
Accepted: July 1, 2021
Published: August 20, 2021

Citation: Jiang Y, Li S, Xiao X, Sun W, Zhang Q. Genotype-phenotype of isolated foveal hypoplasia in a large cohort: Minor iris changes as an indicator of *PAX6* involvement. *Invest Ophthalmol Vis Sci.* 2021;62(10):23.
https://doi.org/10.1167/iovs.62.10.23

Purpose. Foveal hypoplasia (FVH) is defined as the lack of fovea with a relatively preserved neuroretina, occurring either as an isolated FVH (IFVH) condition or associated with other diseases. This study aimed to systemically molecularly characterize IFVH.

Methods. Genetic defects in 33 families with IFVH were analyzed by exome sequencing. Variants in three genes (*PAX6*, *SLC38A8*, and *AHR*) were selected and evaluated with multistep bioinformatic tools.

Results. Mutations in the three genes were identified in 69.7% (23/33) of families with IFVH and infantile nystagmus, including 18 families with *PAX6* mutations, 5 with *SLC38A8* mutations, but none with *AHR* mutations. Clinical data from 32 patients in the 23 families showed FVH, infantile nystagmus, and full iris. Careful follow-up visits revealed subtle changes in iris in 9 of 14 patients with *PAX6* variants. The *PAX6* variants of the 18 families (15 missense and one stop-loss) were mostly located in the C-terminal region of the paired box domain. Variants in *AHR*, *SLC38A8*, and *PAX6* contributed to IFVH in one (2%), 25 (45%), and 30 (53%) families with identified genetic defects (23 families in this study and 33 reported previously), respectively.

Conclusions. *PAX6* and *SLC38A8* mutations are the main cause of IFVH based on our data and a systematic review. IFVH-associated *PAX6* variants are mostly missense with a specific location, indicating a specific correlation of these variants with IFVH but not with typical aniridia. Full iris with subtle structural abnormalities is more common in patients with *PAX6*-associated IFVH, suggesting a potential diagnostic indicator.

Keywords: foveal hypoplasia, infantile nystagmus, *PAX6*, *SLC38A8*, genotype–phenotype

Foveal hypoplasia (FVH) is defined as the underdevelopment of the foveal depression with a relatively preserved neuroretina.[1] The features of FVH include the absence of the foveal pit and foveal avascular zone, the continuity of inner retinal layers, and retinal vessels extending across the presumed foveal area observed by fundus photography or optical coherence tomography.[2,3] It can be an isolated FVH (IFVH)[4–7] entity with infantile nystagmus as its presenting sign. However, it is most commonly accompanied by other ocular or systemic diseases, such as ocular or oculocutaneous albinism,[8] aniridia,[9] optic nerve hypoplasia,[10,11] achromatopsia,[12] or Stickler syndrome.[13]

IFVH is always accompanied by infantile nystagmus and variable degrees of reduced visual acuity but other ocular structures remain relatively normal. Based on the genetic basis, three different types of IFVH have been reported, including the autosomal dominant form of FVH1 due to *PAX6* variants[5,14] and autosomal recessive forms of FVH2 and FVH3 due to variants in *SLC38A8*[15] or *AHR*.[7] However, the contributions of the three genes to IFVH have not been systemically analyzed. In addition, the molecular basis underlying IFVH due to *PAX6* variants is largely unknown, as *PAX6* variants have mostly been detected in patients with aniridia and other associated phenotypes.

In the current study, potential pathogenic variants were detected in 23 of 33 Chinese families with IFVH, including 18 families with heterozygous variants in *PAX6* and five with biallelic variants in *SLC38A8*, but none in *AHR*. In total, variants in *AHR*, *SLC38A8*, and *PAX6* contributed to IFVH in 2%, 45%, and 53% of families with identified genetic defects, respectively, based on 23 IFVH families from this study and 33 IFVH families reported in the literature. Comparative bioinformatics analysis of *PAX6* variants revealed that the IFVH-associated *PAX6* variants were mostly missense and were frequently located in a specific region of the paired box domain. A careful re-evaluation of the iris for patients with *PAX6*-associated IFVH revealed subtle changes in the iris in nine of 14 patients, suggesting a potential diagnostic indicator. These data may enrich our understanding of the molecular mechanism of IFVH.

Methods

Patients and Sample Collection

Probands with IFVH, infantile nystagmus, and complete iris from 33 families were recruited from the Pediatric and Genetic Clinic of the Zhongshan Ophthalmic Center. This

study was performed following the guidelines of the Declaration of Helsinki and approved by the Institute Review Board of the Zhongshan Ophthalmic Center. Prior to collecting clinical data and blood samples, signed informed consent was obtained from all the participants or their guardians. Genomic DNA was prepared from leukocytes of peripheral venous blood.

The probands and their family members underwent routine eye examination. Specific ophthalmologic examinations were performed when applicable, including photography of the anterior segment and/or fundus, optic coherence tomography (OCT), and electroretinogram (ERG).

Variant Detection and Filtering

Targeted exome sequencing or whole-exome sequencing was performed on genomic DNA from the 33 probands according to the previously described procedures.[16,17] Variants in genes associated with nystagmus were filtered according to the following bioinformatics steps described previously.[18] First, synonymous variants and noncoding variants that did not alter any splicing sites predicted by the Berkeley Drosophila Genome Project (https://www.fruitfly.org/) were excluded. Second, variants with a minor allele frequency ≥0.01 according to the Genome Aggregation Database (gnomAD) were excluded. The remaining variants underwent predictions through multiple bioinformatics tools: SIFT (http://sift.jcvi.org/), Polyphen-2 (http://genetics.bwh.harvard.edu/pph2/), PROVEAN (http://provean.jcvi.org/seq_submit.php), CADD (http://cadd.gs.washington.edu), and REVEL (https://sites.google.com/site/revelgenomics/). Then, after comparison with the distribution of variants in gnomAD, the potential pathogenic variants were screened.

Sanger Sequencing

Potential pathogenic variants were validated by Sanger sequencing, using primers designed with the online tool Primer3 (Supplementary Table S1). Segregation analysis was further performed on the available family members. Amplification, sequencing, and target sequence analysis were performed according to previously described procedures.[19]

Computer Modeling and DNA-Protein Interaction Prediction

The obtained protein 3D structures of *PAX6* included an X-ray crystal structure of the DNA-bound paired domain (PDB:6pax) and a homology model of the DNA-bound homeodomain, modeled by the SWISS-MODEL program[20] according to the template of the crystal structure of the highly related Aristaless homeodomain in *Drosophila* (PDB:3lnq). The effects of DNA-protein interactions were predicted with the program FoldX. In accordance with previously reported threshold,[21] a Gibbs free energy gap difference ($\Delta\Delta G = \Delta\Delta G_{mut} - \Delta\Delta G_{wt}$) of a protein monomer that was >1.6 kcal/mol was considered to indicate "destabilizing folding." When variants showed a protein monomer $\Delta\Delta G \leq 1.6$ kcal/mol and the ΔΔG difference gap between the protein monomer and protein:DNA complex was >0.25 kcal/mol, it was considered to indicate "perturb protein:DNA interaction." The other variants were considered to have "unknown molecular effect."

Table 1. Rare Variants in *PAX6* or *SCL38A8* Predicted to be Potentially Damaging

Variants	Exon	Position at chr	Nucleotide Acid change	Amino Acid Effect	REVEL Score	CADD Score	SIFT Score	Polyphen-2 Score	PROVEAN Pred	GnomAD Allele	Family ID	HGMD
A. *PAX6* (chr11, NM_000280.5)												
1	5	31824280	c.113G>C	p.Arg38Pro	0.959	29.2	D (0.001)	PD (0.998)	D	/	7822	DM
2	5	31824265	c.128C>T	p.Ser43Phe	0.963	28.5	D (0.000)	PD (0.999)	D	/	8407	DM
3	6	31823324	c.142G>A	p.Val48Met	0.952	32	D (0.000)	PD (1.000)	D	/	8453	/
4	6	31823324	c.142G>T	p.Val48Leu	0.968	33	D (0.001)	PD (1.000)	D	/	8465	/
5	6	31823252	c.214G>T	p.Gly72Cys	0.984	31	D (0.000)	PD (1.000)	D	1/31404	4012	DM
6	6	31823252	c.214G>A	p.Gly72Ser	0.974	29.2	D (0.001)	PD (0.995)	D	/	16526	DM
7	6	31823237	c.229A>G	p.Arg77Gly	0.936	24.8	D (0.000)	PD (0.981)	D	/	5538	/
8	6	31823233	c.233T>G	p.Val78Gly	0.566	27.9	D (0.000)	PD (1.000)	D	/	14014	DM
9	6	31823231	c.235G>C	p.Ala79Pro	0.594	27.4	D (0.001)	PD (0.998)	D	/	17508	/
10	6	31823170	c.296C>T	p.Ala99Val	0.950	28.8	D (0.001)	PD (0.999)	D	/	20011	/
11	7	31822404	c.358G>A	p.Val120Met	0.891	32	D (0.000)	PD (1.000)	N	/	10675	/
12	7	31822379	c.383G>T	p.Arg128Leu	0.908	24.6	D (0.000)	B (0.280)	D	/	17516	/
13	7	31822379	c.383G>A	p.Arg128His	0.933	28.1	D (0.000)	PB (0.773)	D	/	18734	/
14	8	31816238	c.622C>T	p.Arg208Trp	0.877	29.4	D (0.000)	PD (1.000)	D	1/251466	7721; 6565	DM
15	10	31815345	c.771G>T	p.Trp257Cys	0.956	32	D (0.000)	PD (1.000)	D	/	17267	/
16	13	31811483	c.1268A>T	p.*423Leuext*14	/	/	/	/	/	/	14860; 4926	DM
B. *SLC38A8* (chr16, NM_001080442.3)												
1	2	84075752	c.11delA	p.Gln4Argfs*31	/	/	/	/	/	/	15394	/
2	6	84063109	c.680T>A	p.Phe227Tyr	0.647	29.4	D (0.000)	PD (1.000)	D	53/282750	4517	/
3	6	84063107	c.682G>C	p.Gly228Arg	0.625	28.9	D (0.001)	PD (1.000)	D	5/282722	141	/
4	6	84063100	c.689A>G	p.Gln230Arg	0.532	33	D (0.004)	PD (1.000)	D	/	141	/
5	7	84056488	c.697G>A	p.Glu233Lys	0.792	25.6	T (0.245)	PD (1.000)	N	20/266328	15394;14534;20140	DM†
6	10	84046650	c.1170C>A	p.Cys390*	/	/	/	/	/	/	4517	/

Note: For *PAX6* in gnomAD, 5% variants had REVEL or CADD scores greater than 0.88 or 29.9, while 75% had such scores less than 0.61 or 24.

For *SLC38A8* in gnomAD, 5% variants had REVEL or CADD scores greater than 0.56 or 28.4, while 75% had such scores less than 0.34 or 24.2.

PD = probably damaging; PB = possibly damaging; D = damaging; B = benign; T = tolerant; N = neutral; DM = damaging mutation; PolyPhen-2 version 2.2.2.

† The c.697G>A is a well-defined pathogenic variant reported in previous study (Poulter JA, et al. Am J Hum Genet 2013;93:1143-1150).

Investigative Ophthalmology & Visual Science

Review of IFVH-Related Variants in *PAX6*, *SLC38A8*, and *AHR*

We conducted searches with the keywords "*PAX6*," "*SLC38A8*," "*AHR*," "isolated foveal hypoplasia," and "idiopathic infantile nystagmus" in the PubMed (https://www.ncbi.nlm.nih.gov/pubmed/), Google Scholar (http://so.hiqq.com.cn/), and collected available related references in English. Additionally, we collected the variants in *PAX6*, *SLC38A8*, and *AHR* related to IFVH or infantile nystagmus with IFVH and associated available references from the Human Gene Mutation Database (HGMD) on January 22, 2021. Accordingly, we summarized the numbers of different variants in the three genes, the frequency of variants in affected individuals or pedigrees, the distribution of variants in mRNA, and genotype-phenotype correlations.

Results

Mutation Detection

Based on the multistep bioinformatics analysis, potential pathogenic variants were detected in 23 of the 33 probands with IFVH by exome sequencing, including 16 heterozygous variants in *PAX6* in 18 families and homozygous or compound heterozygous variants in *SLC38A8* in 5 families (Table 1). These variants were confirmed by Sanger sequencing (Supplementary Fig. S1) and were shown to be transmitted with IFVH in the segregation analysis conducted in available family members (Fig. 1; Table 2). Among the 16 variants in *PAX6*, 15 were missense variants (nine novel) and one was a known stop-loss variant (c.1268A>T/p.*423Leuext*14). Among the 15 missense variants in *PAX6*, 13 were located in a paired box domain

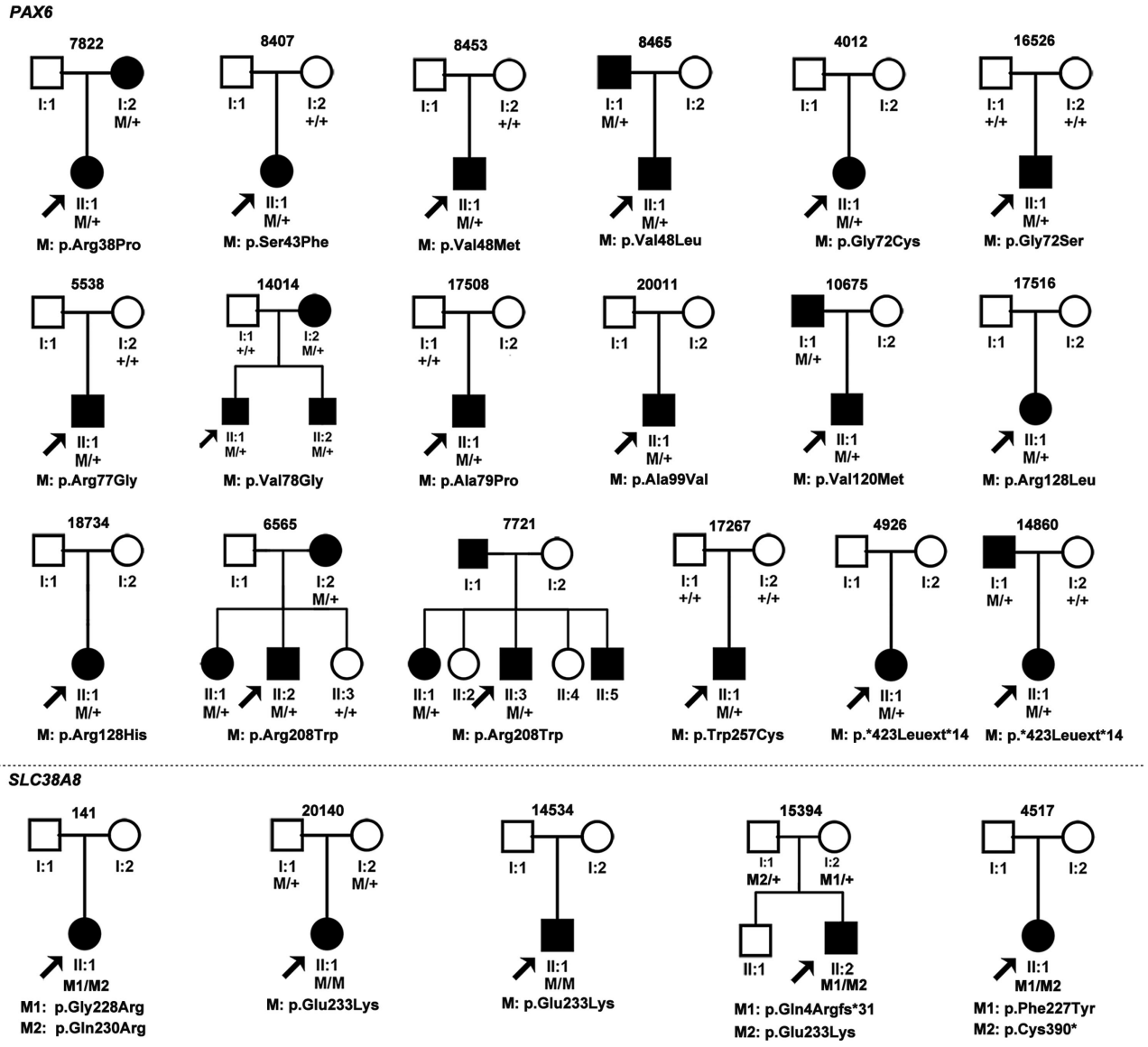

Figure 1. The pedigrees of 18 families with potential pathogenic variants in *PAX6* and five families with potential pathogenic variants in *SLC38A8* in our cohort. The variants of the probands and family members are provided below the pedigrees. M points at the variant site, + points at normal allele. The filled shapes including square patterns (male) and circle patterns (female) represent the affected patients. The pedigrees with *PAX6* variants are shown above the dotted line and the pedigrees with *SLC38A8* variants are below the dotted line.

Table 2. Clinical Information of the Probands and Affected Siblings With *PAX6* or *SLC38A8* Variants Identified in this Study

Family ID	Nucleotide Acid Change	Amino Acid Effect	Gender	Age (Years) At Exam	Initial Symptom	Visual Acuity OD; OS	OCT Grade	Fundus
A. *PAX6* (accession number NM_000280.5)								
7822-II:1	c.113G>C	p.Arg38Pro	F	0.4	NYS	NA; NA	NA	AFM
8407-II:1	c.128C>T	p.Ser43Phe	F	4	NYS	NA; NA	NA	AFM
8453-II:1	c.142G>A	p.Val48Met	M	2.8	NYS	0.05*; 0.05*	NA	AFM; VAA
8465-I:1	c.142G>T	p.Val48Leu	M	38	NYS	0.08; 0.3	NA	FVH
8465-II:1	c.142G>T	p.Val48Leu	M	4	NYS	NA; NA	NA	AFM
4012-II:1	c.214G>T	p.Gly72Cys	F	7	NYS	0.1; 0.1	NA	AFM; VAA; TF
16526-II:1	c.214G>A	p.Gly72Ser	M	4	NYS	NA; NA	NA	AFM; VAA; TF; ODH
5538-II:1	c.229A>G	p.Arg77Gly	M	1.2	NYS	NA; NA	Grade 3 FVH	AFM; VAA
14014-I:2	c.233T>G	p.Val78Gly	F	30	NYS	0.1; 0.05	Grade 3 FVH	AFM; TF
14014-II:1	c.233T>G	p.Val78Gly	M	6	NYS	0.1; 0.05	Grade 3 FVH	DFM, VAA, TF
14014-II:2	c.233T>G	p.Val78Gly	M	5	NYS	NA; NA	NA	AFM; VAA; TF
17508-II:1	c.235G>C	p.Ala79Pro	M	2	NYS	0.1*; 0.15*	NA	AFM; VAA; TF
20011-II:1	c.296C>T	p.Ala99Val	M	22	NYS	0.2; 0.2	Grade 3 FVH	AFM; VAA
10675-I:1	c.358G>A	p.Val120Met	M	37.7	NYS	NA; NA	Grade 3 FVH	FVH
10675-II:1	c.358G>A	p.Val120Met	M	6.8	NYS	0.6; 0.3	Grade 3 FVH	AFM, VAA, TF
17516-II:1	c.383G>T	p.Arg128Leu	F	6.2	NYS	0.2; 0.2	Grade 3 FVH	AFM; VAA
18734-II:1	c.383G>A	p.Arg128His	F	12.3	NYS	0.3*; 0.3*	NA	AFM
6565-I:2	c.622C>T	p.Arg208Trp	F	62	NYS	0.5; 0.5	Grade 1 FVH	DFM; ODH (OD)
6565-II:1	c.622C>T	p.Arg208Trp	F	36	NYS	FC; 0.4	Grade 1 FVH	DFM, ODH (OS)
6565-II:2	c.622C>T	p.Arg208Trp	M	31	NYS	0.1; 0.2	Grade 1 FVH	AFM; ODH; VAA
7721-II:1	c.622C>T	p.Arg208Trp	M	28	NYS	0.05; 0.05	NA	DFM; ODH; VAA
7721-II:3	c.622C>T	p.Arg208Trp	F	36	NYS	0.02; 0.05	NA	DFM; VAA; TF; ODH
17267-II:1	c.771G>T	p.Trp257Cys	M	5	NYS	0.5; 0.5	Grade 3 FVH	AFM; ODH; VAA
4926-II:1	c.1268A>T	p.*423Leuext*14	F	6	NYS	0.1; 0.1	Grade 3 FVH	AFM, VAA
14860-I:1	c.1268A>T	p.*423Leuext*14	M	29	NYS	0.2; 0.2	NA	FVH
14860-II:1	c.1268A>T	p.*423Leuext*14	F	4	NYS	NA; NA	Grade 3 FVH	AFM, VAA, TF
B. *SLC38A8* (accession number NM_001080442.3)								
141-II:1	c.[682G>C]; [689A>G]	p.[Gly228Arg]; [Gln230Arg]	F	1	NYS	NA; NA	NA	AFM; TF
20140-II:1	c.[697G>A]; [697G>A]	p.[Glu233Lys]; [Glu233Lys]	F	0.5	NYS	NA; NA	Grade 3 FVH	AFM; TF; ODH
14534-II:1	c.[697G>A]; [697G>A]	p.[Glu233Lys];[Glu233Lys]	M	23	NYS	0.03; 0.15	NA	AFM; TF; ODH
15394-II:2	c.[11delA]; [697G>A]	p.[Gln4Argfs*31]; [Glu233Lys]	M	0.3	NYS	NA; NA	Grade 3 FVH	AFM; TF
4517-II:1	c.[680T>A]; [1170C>A]	p.[Phe227Tyr]; [Cys390*]	F	5.7	NYS	0.1; 0.15	NA	AFM; TF

Notes: The above data based on available clinical data from patients. All patients had full iris.

M = male; F = female; OCT = optical coherence tomography; NA = not available; NYS = nystagmus; HM = high myopia; FC = finger counting; FVH = foveal hypoplasia; TF = tessellated fundus; VAA = vascular arcades abnormalities; AFM = absent foveal reflex and macular pigment; DFM = decreased foveal reflex and macular pigment; ODH = optic disk hypoplasia.

*The visual acuity examination was performed on the proband 8453-II:1 at the age of 4 years, 17508-II:1 at the age of 5 years, and 18734-II:1 at the age of 24 years.

and one was located in a homeobox domain. Interestingly, among these 15 variants, nine were predicted to perturb the interaction with DNA, four were predicted to be destabilizing and disrupt protein folding, and two had an unknown molecular effect (Supplementary Table S2). In addition, the biallelic variants in *SLC38A8* identified in five families involved six variants, five of which were novel, whereas the remaining variant, c.697G>A/p.Glu233Lys, was previously reported[6] (see Table 1). Among the five families with variants in *SLC38A8*, two had the same homozygous variants (c.697G>A/p.Glu233Lys) and three had compound heterozygous variants (see Table 2). All of these variants were either predicted to be damaging or shown to be causative in previous studies. In addition, mutations in other genes associated with syndromic FVH or nystagmus, including hemizygous or heterozygous damaging variants in *FRMD7* associated with idiopathic infantile nystagmus or those in *GPR143* associated with ocular albinism, biallelic variants in genes contributed to autosomal recessive oculocutaneous albinism (arOCA; such as *AP3B1*, *AP3D1*, *BLOC1S3*, *BLOC1S6*, *C10ORF11*, *DTNBP1*, *GPR143*, *HPS1*, *HPS3*, *HPS4*, *HPS5*, *HPS6*, *OCA2*, *SLC24A5*, *SLC45A2*, *TYR*, and *TYRP1*), as well as potential pathogenic variants in other genes associated with retinal degeneration listed in RetNet (https://sph.uth.edu/retnet/), were excluded in the 23 families. However, single heterozygous variants in genes known to contribute to arOCA were detected in 12 of 33 families (Supplementary Table S5), but these variants are unlikely to contribute to the diseases because none of the heterozygous carriers with arOCA had FVH or nystagmus in the published literature and in our cohort (data unpublished).

The Characteristics of the Clinical Phenotypes

Among the 32 patients with mutations from the 23 families, clinical data were available for further analysis in all but one patient, including 26 patients from 18 families with variants in *PAX6* and five patients from five families with variants in *SLC38A8* (see Table 2). In all of the patients with identified mutations, nystagmus was noted as an initial presenting symptom, whereas FVH was recorded as the major finding upon fundus examination.

Among the five patients with biallelic variants in *SLC38A8*, the initial symptom was horizontal nystagmus and the best corrected visual acuity was 0.15 in two patients. All five patients showed clear evidence of FVH, with the absence of a foveal reflex and macular hyperpigmentation. Moreover, a tessellated fundus was found in all patients. Accordingly, the OCT results revealed grade 3 FVH (Figs. 2J–L; Figs. 3G, 3H).

Investigative Ophthalmology & Visual Science

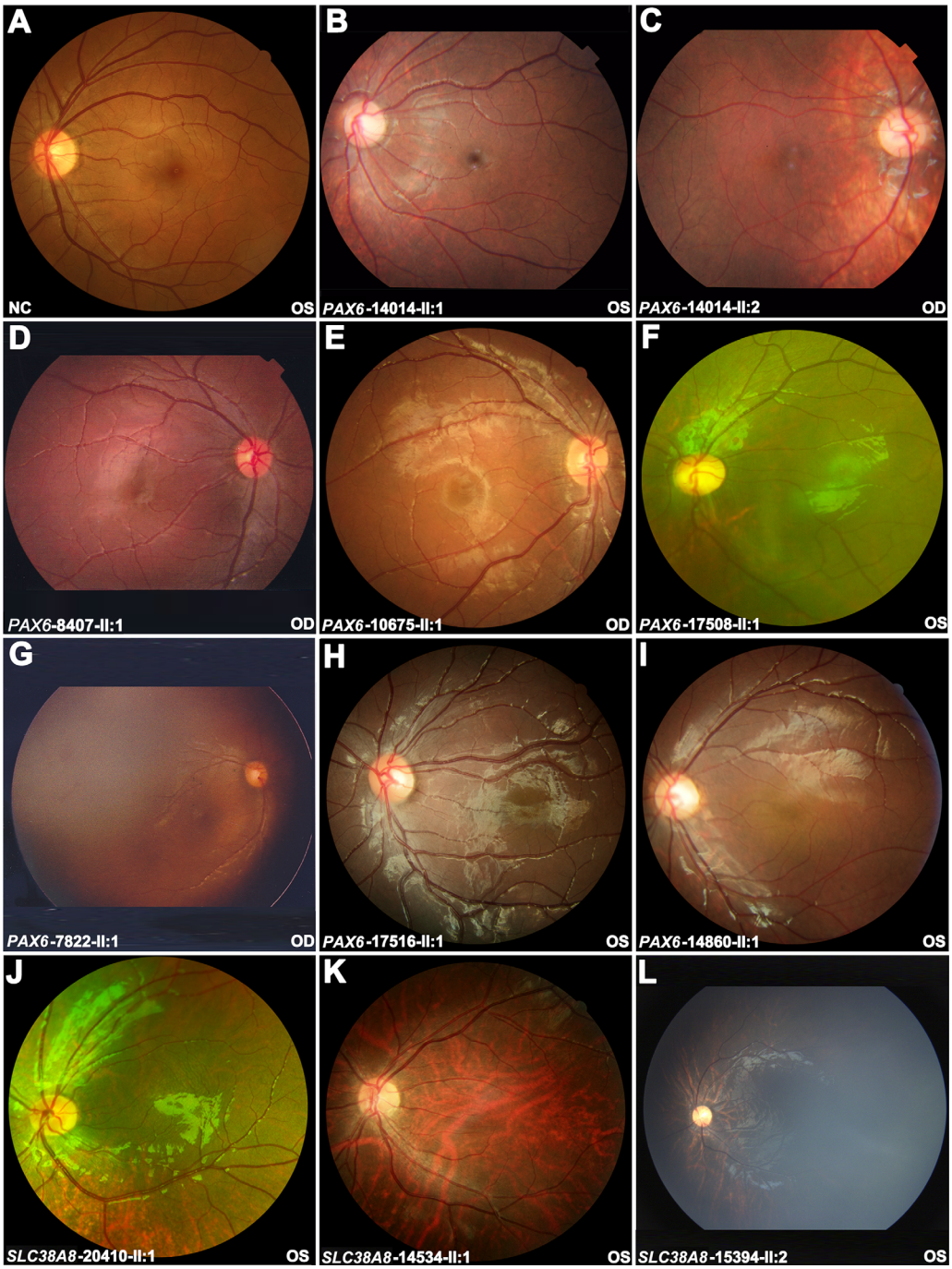

Figure 2. Representative fundus photographs from patients with isolated foveal hypoplasia. (**A**) Normal fundus photography of an unrelated normal control. (**B**) The fundus photograph of a patient with *PAX6* variants (14014-II:1) shows that the blunting fovea reflex and decreased macular hyperpigmentation. A tessellated fundus and the retinal vasculature crossing the foveal avascular area are observed. (**C–I**) The absence of a foveal pit including the lack of a foveal reflex and macular hyperpigmentation are observed in all the patients with *PAX6* variants. In four patients (14014-II:2, 17508-II:1, 17516-II:1, and 14860-II:1), the fundus images show the retinal vasculature crossing the foveal avascular zone. The fundus photographs of four patients (14014-II:2, 10675-II:1, 17508-II:1, and 14860-II:1) showing tessellated fundus changes below the optic disc. (**J–L**) Fundus photographs from patients with *SLC38A8* variants showing a tessellated fundus and the lack of a foveal pit.

The main type of nystagmus observed in the 26 patients with *PAX6* variations was conjugate horizontal pendular nystagmus in 12 patients. In addition to the observation of unclassified nystagmus in 11 patients, the other types of nystagmus oscillations recorded included vertical oscillations in one patient, torsional oscillations in one patient, and multiplanar oscillations (horizontal, vertical, and torsional) in one patient. For the 26 patients with variation in *PAX6*, the best corrected visual acuity ranged from a Snellen equivalent of 0.05 to 0.6 (Supplementary Fig. S2), with the majority (66.7%) having a visual acuity below 0.3. The recorded refractive errors included myopia (10 eyes with low myopia,

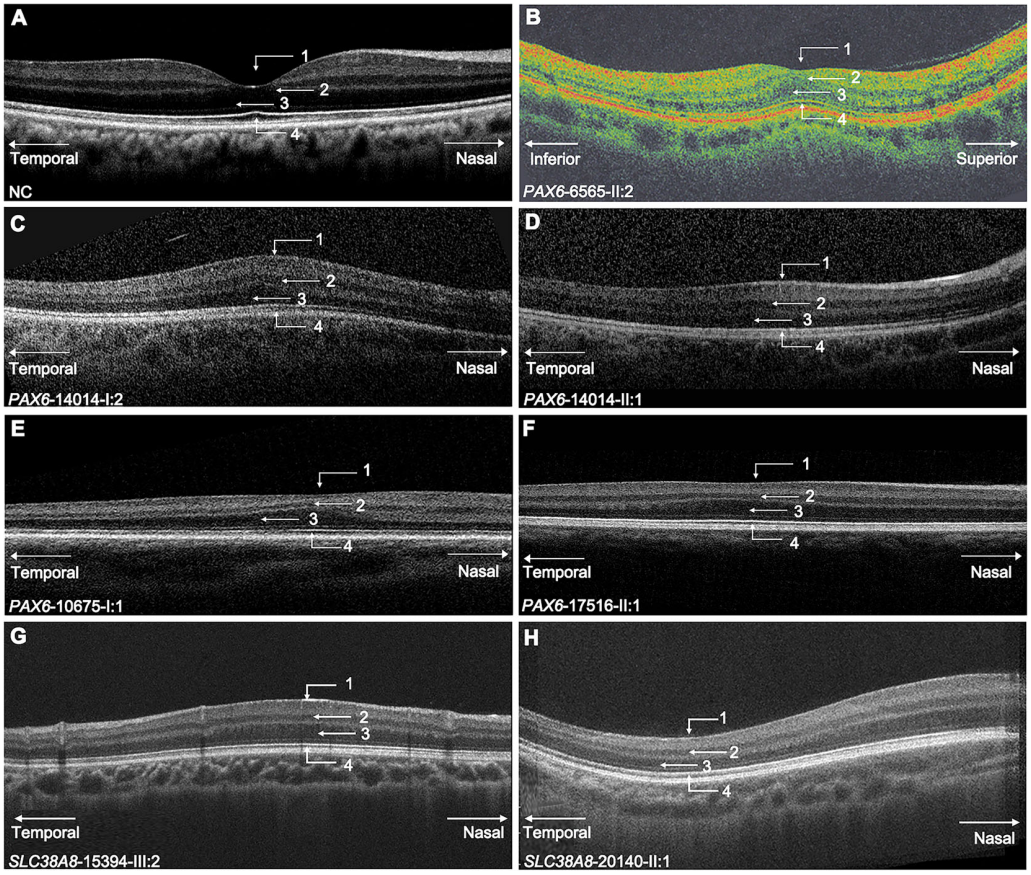

Figure 3. Optical coherence tomography (OCT) scans through the fovea of patients with *PAX6* or *SLC38A8* variants. (**A**) A normal OCT scan through the fovea in an unrelated normal control. (**B**) The OCT image of grade 1 fovea hypoplasia from a patient with *PAX6* variant (6565-II:2) are shown as the following points: the shallow fovea pit (1), intrusion of plexiform layers (2), outer nuclear layer widening (3), and outer segment lengthening (4). (**C–F**) OCT images of grade 3 foveal hypoplasia from patients with *PAX6* variants (14014-I:2, 14014-II:1, 10675-I:1, and 17516-II:1) showing the following: the absence of a foveal pit (1), intrusion of plexiform layers (2), outer nuclear layer widening (3), and absence of outer segment lengthening (4). (**G, H**) OCT scans of grade 3 foveal hypoplasia from patients with *SLC38A8* variants (15394-II:2 and 20140-II:1).

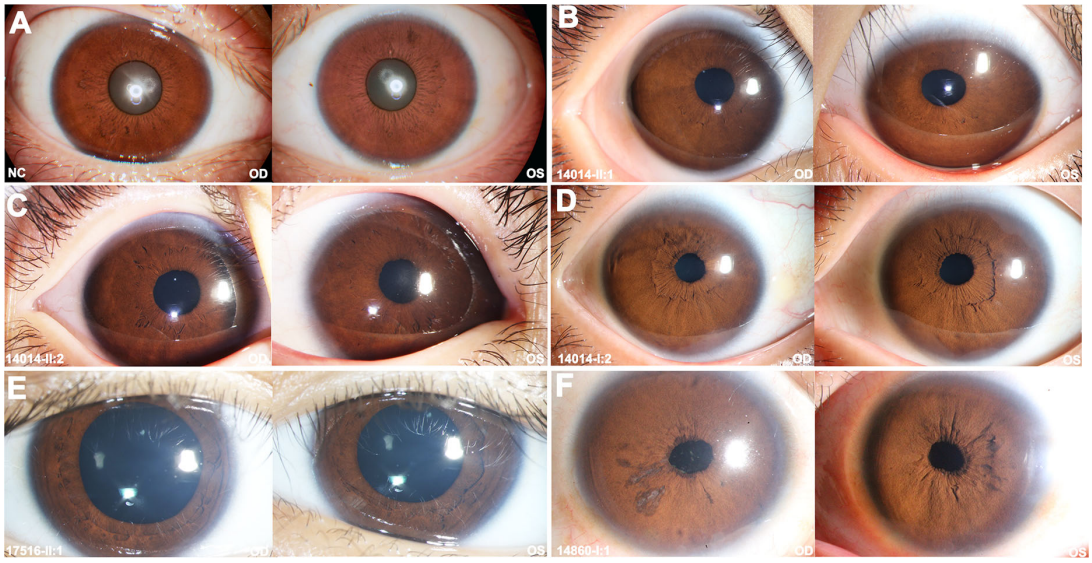

Figure 4. Ocular anterior segment photographs of the patients with *PAX6* variants. (**A**) The normal complete iris surface of an unrelated normal control. (**B–C**) The iris appearance demonstrates full iris but subtle structural changes, including a smooth surface without details, such as crypts and contraction furrows, in both eyes from two patients (14014-II:1 and 14014-II:2). The collarette area is unobvious. (**D**) Iris photography from a patient (14014-I:2) showing a velvety surface with a lack of crypts and contraction furrows, a predominant collarette and a distorted pupillary ruff. (**E**) The iris of another patient (17516-II:1) showing an unobvious collarette area and crypts. (**F**) The image of the iris shows the absence of a collarette area, crypts, and contraction furrows in the patient (14860-I:1). The distortion of the pupillary ruff can also be observed.

Investigative Ophthalmology & Visual Science

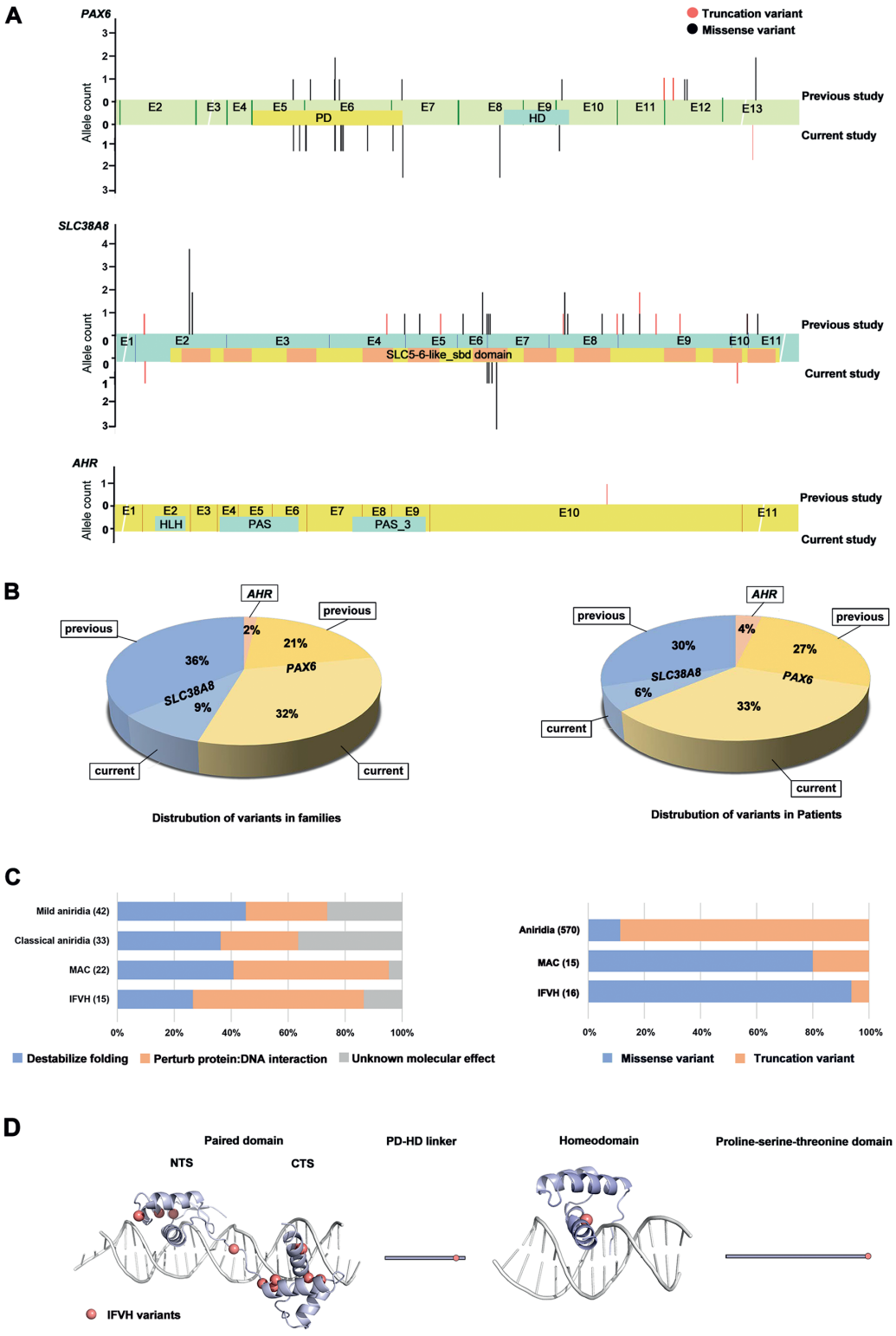

Figure 5. The distribution, protein structure analysis and DNA interaction prediction of *PAX6* variants. (**A**) The allele count and distribution of *PAX6*, *SLC38A8*, and *AHR* variants in mRNA sequences found in previous studies and in-house data (Ref. NM_000280.5; NM_001080442.3; and NM_001621.4). The variants reported in previous studies are positioned above the sequence, whereas the variants in our cohort are positioned below the sequence. More of the *PAX6* variants related to isolated foveal hypoplasia with infantile nystagmus were located in the C-terminal subdomain than in the N-terminal subdomain of the paired domain. (**B**) The distribution of *PAX6*, *SLC38A8*, and *AHR* variants in the current study and previous literature. The sector diagram showed the frequency of variants in the three genes identified in previous studies and our cohort among families and patients. (**C**) The distribution of *PAX6* variants associated with different phenotypes. The left panel shows the results of molecular effect prediction for *PAX6* missense variants associated with different phenotypes in our cohort and previous reports (Ref. Williamson KA, et al. Genet Med 2020; 22(3): 598-609). More than half of the variants associated with isolated foveal hypoplasia were predicted to perturb the interaction with DNA. The right panel shows the distribution of different variant types associated with different phenotypes in the HGMD and our cohort. Missense variants in *PAX6* associated with isolated foveal

Investigative Ophthalmology & Visual Science

hypoplasia were obviously more common than truncation variants, which differs from the distribution of variant types related to aniridia. (**D**) Protein analysis of *PAX6* missense variants related with isolated foveal hypoplasia. Most of the potential pathogenic variants identified in our cohort were located in the C-terminal subdomain of the paired domain.

3 eyes with moderate myopia, and 16 eyes with high myopia), and hyperopia (5 eyes with low hyperopia, 2 eyes with moderate hyperopia, and 3 eyes with high hyperopia). The ERGs of four patients with *PAX6* mutations demonstrated mild-to-moderate, moderate, moderate-to-severe, and severe reduction of cone and rod responses in each of the four, respectively. FVH was present in all 26 patients, including a lack or abnormality of the following signs: foveal pit, foveal reflex, yellowish macular area, avascular zone, and normal macular vascular arcades (see Table 2; Fig. 2). FVH was clearly demonstrated by available OCT scans in 26 eyes of 13 patients (see Fig. 3; Table 2), in whom 20 eyes in 10 patients were classified as grade 3 FVH, whereas six eyes in three patients were classified as grade 1 FVH.[3]

As aniridia or partial iris defects have been well recognized as the main feature associated with most mutations in *PAX6*, it was of interest to investigate whether there were any noticeable subtle changes in the full iris of those patients with IFVH and *PAX6* variants. Therefore, careful observations of the iris were performed in 14 patients with IFVH with *PAX6* mutations during follow-up visits. The reexamination of the anterior segment demonstrated a normal cornea in all 14 patients, but subtle and noticeable anomalies of the iris in nine of the 14 patients. The iris changes observed in the nine patients included the absence of crypts and contraction furrows in all nine patients, the lack of a collarette in eight patients, a distorted pupillary ruff in three patients, and a predominant collarette in one patient (Fig. 4, Supplementary Table S3). Mild corectopia was observed in five of the 14 patients and one patient had a persistent pupillary membrane.

The Spectrum of Variants in *PAX6*, *SLC38A8*, and *AHR* Related to IFVH

Previously, 39 variants in the three genes were reported in 49 patients from 33 families (Supplementary Table S4).[5–7,14,15,22–31] In the current study, 22 potential pathogenic variants (PPVs) in two of the three genes were detected in 32 patients from 23 families. So far, our cohort represents 41% of currently reported families and 39% of currently reported patients with a confirmed genetic diagnosis of IFVH (see Fig. 5B). Overall, variants in *AHR*, *SLC38A8*, and *PAX6* contributed to one (2%), 25 (45%), and 30 (53%) of families with a genetic diagnosis of IFVH, respectively, based on our current cohort and previous reports in the literature. Of these, the variants in *PAX6* contributing to IFVH were located mostly within the C-terminal subdomain of the paired box domain (see Figs. 5A, 5D). In addition, the variants in *SLC38A8* identified in our cohort were located mainly in transmembrane domain 6. Although no *AHR* variants were identified in our cohort, the sole reported truncation variant was located in exon 10 (see Fig. 5A).

Discussion

In this study, 16 PPVs in *PAX6* and 6 PPVs in *SLC38A8* were identified in 23 of 33 probands with IFVH and infantile nystagmus. Based on the 33 previously reported families with IFVH and infantile nystagmus, the contribution of variants in *SLC38A8* (61%) was considered to be greater than those of *PAX6* (36%) and *AHR* (3%). However, the proportion changes when our cohort combined with previous reports, where variants in *PAX6* (53%) are more common for IFVH and infantile nystagmus than those in *SLC38A8* (45%) or *AHR* (2%). Additionally, our cohort indicates that variants in the *PAX6* and *SLC38A8* can be considered as the common cause for IFVH and as the prioritized targets in clinical gene test for patients with IFVH.

For *PAX6*, 16 variants are considered as PPVs contributed to IFVH and infantile nystagmus. Several lines of evidence listed below support such association. (1) These 15 missense variants and one stop-loss variant are present exclusively in these families and most of them are absent in the gnomAD. (2) These PPVs are predicted to be damaging by multiple in silico bioinformatics tools (see Table 1), suggesting that these have an effect on the development of diseases. (3) They segregate with the phenotype in most families (4) Among the 15 missense variants, 13 are located in the paired box domain (PD) and one in the homeodomain (HD). The remaining one, located in the linker region between the two domains, has been identified as a pathogenic variant associated with aniridia and non-aniridia phenotypes in previous studies.[32,33] The PD consists of N-terminal (NTS) and C-terminal subdomains (CTS), that can bind the consensus DNA sequences and influence the DNA-binding effect of the HD.[34] Based on the distribution of variants in the three-dimension protein structure and mRNA sequence (Fig. 5D), missense variants contributed to IFVH in our cohort are mostly located in CTS, similar to previous reports.[5,14,35] In comparison, missense variants contributed to aniridia, microphthalmia, anophthalmia, and coloboma are mainly located in NTS.[21] Additionally, over half of the missense variants identified in our study were predicted to perturb the interaction with DNA. However, in a previous study,[21] aniridia variants were predicted to destabilize the protein folding to a greater extent than perturb the interaction with DNA. Likewise, according to the HGMD and our cohort, the missense variants were more common than truncation variants in patients with IFVH or MAC (94% and 80%, respectively). In contrast, the truncation variants were identified in more than 80% of aniridia patients (see Fig. 5C). (5) The stop-loss variant (c.1268A>T/p.*423Leuext*14), predicted to induce C-terminal extension (CTE), is a known pathogenic variant for aniridia, absents in gnomAD, and co-segregates with IFVH of three families in our cohort (Supplementary Fig. S1). In previous studies, different CTE variants have been identified in 10 patients with FVH accompanied with or without additional abnormalities in anterior segment.[23] Accordingly, all three patients with the stop-loss variant in our cohort had full iris with subtle structure changes. Similar to previous studies,[23,35] the iris abnormalities observed in patients with the CTE variant were more severe than those in patients with missense variants in our cohort.

Variants in *PAX6* contributed to at least nine different phenotypes with aniridia as the main entity (OMIM 607108). Based on previous reports and our current study, truncation variants are usually associated with aniridia, whereas

Investigative Ophthalmology & Visual Science

missense variants located in CTS are frequently related to IFVH. Besides, overlapping phenotypes caused by the same class of variants have been occasionally observed,[23,36,37] suggesting that other factors may also contribute to the phenotypic diversity in addition to the variants themselves, such as mosaicism,[38] gene dosage,[39] modified factors (genetic, epigenetic, or environmental),[22] and pleiotropy.[40] Further studies on the mechanism of phenotypic variability will be valuable for the treatment of eye anomalies associated with *PAX6* variants. Contrary to the missense variants associated with aniridia mainly located in the NTS of PD, however, IFVH associated with specific enrichment of missense variants at CTS[35] indicates that the CTS region may play an important role in the fine regulation of fovea development and ganglion cell axon projection but may not be critical for iris development. There is a negative interaction of transcription activity between CTS and NTS.[5,41,42] The CTS of PD has been previously suggested to independently modulate the DNA-binding ability of the PAX6(5a) isoform, which is the alternative splicing of PAX6 and characterized by the insertion of 14 amino acid encoded by exon 5a in the PD. A previous study reported that PAX6(5a) isoform expression might contribute to the induction of cascades in retina development, which led to the formation of the retinal area containing the accumulation of visual cells.[43] The missense variants may disrupt the regulation mechanism described above.[42]

For *SLC38A8* and *AHR*, six variants in *SLC38A8* were identified as PPVs, including five novel and one homozygous missense variant in two families, which has been reported in patients with FVH, optic nerve decussation defects, anterior segment dysgenesis (FHONDA) syndrome.[6] In our cohort, these PPVs in *SLC38A8* were responsible for 15.2% cases. Kuht et al. reported PPVs in *SLC38A8* accounted for the 1.8% (9/511) patients with FVH and nystagmus in their cohort.[30] The higher disease burden caused by *SLC38A8* in our study may be due to exclusion of other ocular systemic diseases accompanied with FVH during the recruitment, such as ocular or oculocutaneous albinism, Stickler syndrome, etc. As for *AHR*, the previous report of only one IFVH family with homozygous nonsense mutation[7] and absence of biallelic variants in our cohort suggest that variant in *AHR* is a rare cause of IFVH.

The etiology of many infantile nystagmus remains unclear, but the available results imply that abnormalities in components of the ocular motor system and afferent visual system are involved in the development of infantile nystagmus.[44] One mechanistic hypothesis explaining this condition involves the miswiring of the visual system.[45,46] The development of infantile nystagmus has also been suggested to be an adaptive response to the lack of high spatial frequency sensitivity due to retinal structural abnormalities, such as FVH, involving the movement of images across the retina to maximize the visual contrast.[47] According to previous studies, in foveal hypoplasia related disorders, such as albinism or aniridia, most patients with foveal hypoplasia had nystagmus.[48,49] However, the FVH is not accompanied by nystagmus in all cases. For example, mild FVH was considered a characteristic of patients with Stickler syndrome.[13] However, nystagmus rarely has been found relationship with Stickler syndrome.[50,51] This gives rise to the hypothesis that the genetic mechanisms rather than foveal structural abnormalities are involved in the development of infantile nystagmus.

Classical aniridia is tightly linked with haploinsufficiency *PAX6*, which is caused by whole-gene deletions, cis-regulatory variants, or premature termination codon causing variants. The missense variants in *PAX6* tend to be associated with milder phenotypes, such as partial aniridia, IFVH, microphthalmia, coloboma, optic nerve defect, and anterior segment dysgenesis.[35] Some studies have reported that the range of iris phenotypes found in some aniridia families includes full iris with subtle iris abnormalities and missense variants in *PAX6* caused full iris with abnormal iris structure.[23,52] Therefore, after PPVs in *PAX6* were detected among the patients with IFVH and infantile nystagmus, the iris of the followed up patients was examined. Interestingly, the available iris photographs show that all patients have full iris with subtle structure changes: velvety surface with few crypts and contraction furrows or without, the absence of or bulge of collarette, and distorted pupillary ruff. Such phenotypes were exclusively observed in these families with PPVs in *PAX6*, which had IFVH with infantile nystagmus. This indicates that an association exists between PPVs in *PAX6* and iris phenotype of patients with IFVH accompanied by infantile nystagmus. This will contribute to diagnosing the IFVH with infantile nystagmus. Thus, when we diagnose patients who show similar iris changes and nystagmus as the initial symptoms, it is necessary to carefully consider the possibility that the patients may have IFVH and may carry PPVs in *PAX6*.

In summary, variants in *PAX6* and *SLC38A8* are considered as the main cause of IFVH. Besides, the genotypic and clinical phenotypic features of patients with IFVH accompanied by infantile nystagmus are systematically analyzed. In this cohort, the occurrence of the complete iris but subtle structural changes are more frequent in patients with *PAX6* variants. This overlooked characteristic will contribute to the diagnosis and management of IFVH with nystagmus.

Acknowledgments

The authors thank to all patients and their family members for participating in this study.

Supported by grants from the Fundamental Research Funds of the State Key Laboratory of Ophthalmology.

Disclosure: **Y. Jiang**, None; **S. Li**, None; **X. Xiao**, None; **W. Sun**, None; **Q. Zhang**, None

References

1. Thomas MG, Kumar A, Mohammad S, et al. Structural grading of foveal hypoplasia using spectral-domain optical coherence tomography a predictor of visual acuity? *Ophthalmology*. 2011;118:1653–1660.
2. Oliver MD, Dotan SA, Chemke J, Abraham FA. Isolated foveal hypoplasia. *Br J Ophthalmol*. 1987;71:926–930.
3. Rufai SR, Thomas MG, Purohit R, et al. Can structural grading of foveal hypoplasia predict future vision in infantile nystagmus?: A longitudinal study. *Ophthalmology*. 2020;127:492–500.
4. Thomas MG, Papageorgiou E, Kuht HJ, Gottlob I. Normal and abnormal foveal development [published online ahead of print November 4, 2020]. *Br J Ophthalmol*, https://doi.org/10.1136/bjophthalmol-2020-316348.
5. Azuma N, Nishina S, Yanagisawa H, Okuyama T, Yamada M. PAX6 missense mutation in isolated foveal hypoplasia. *Nat Genet*. 1996;13:141–142.

6. Poulter JA, Al-Araimi M, Conte I, et al. Recessive mutations in SLC38A8 cause foveal hypoplasia and optic nerve misrouting without albinism. *Am J Hum Genet*. 2013;93:1143–1150.
7. Mayer AK, Mahajnah M, Thomas MG, et al. Homozygous stop mutation in AHR causes autosomal recessive foveal hypoplasia and infantile nystagmus. *Brain: A J Neurol*. 2019;142:1528–1534.
8. Summers CG, King RA. Ophthalmic features of minimal pigment oculocutaneous albinism. *Ophthalmology*. 1994;101:906–914.
9. Hingorani M, Hanson I, van Heyningen V. Aniridia. *Eur J Human Genet: EJHG*. 2012;20:1011–1017.
10. Pilat A, Sibley D, McLean RJ, Proudlock FA, Gottlob I. High-resolution imaging of the optic nerve and retina in optic nerve hypoplasia. *Ophthalmology*. 2015;122:1330–1339.
11. Katagiri S, Nishina S, Yokoi T, et al. Retinal structure and function in eyes with optic nerve hypoplasia. *Sci Rep*. 2017;7:42480.
12. Sundaram V, Wilde C, Aboshiha J, et al. Retinal structure and function in achromatopsia: implications for gene therapy. *Ophthalmology*. 2014;121:234–245.
13. Matsushita I, Nagata T, Hayashi T, et al. Foveal hypoplasia in patients with Stickler syndrome. *Ophthalmology*. 2017;124:896–902.
14. Thomas S, Thomas MG, Andrews C, et al. Autosomal-dominant nystagmus, foveal hypoplasia and presenile cataract associated with a novel PAX6 mutation. *Eur J Human Genet: EJHG*. 2014;22:344–349.
15. Perez Y, Gradstein L, Flusser H, et al. Isolated foveal hypoplasia with secondary nystagmus and low vision is associated with a homozygous SLC38A8 mutation. *Eur J Human Genet: EJHG*. 2014;22:703–706.
16. Wang P, Li S, Sun W, et al. An ophthalmic targeted exome sequencing panel as a powerful tool to identify causative mutations in patients suspected of hereditary eye diseases. *Transl Vis Sci Technol*. 2019;8:21.
17. Li J, Jiang D, Xiao X, et al. Evaluation of 12 myopia-associated genes in Chinese patients with high myopia. *Invest Ophthalmol Vis Sci*. 2015;56:722–729.
18. Xu Y, Guan L, Xiao X, et al. Mutation analysis in 129 genes associated with other forms of retinal dystrophy in 157 families with retinitis pigmentosa based on exome sequencing. *Molecular Vision*. 2015;21:477–486.
19. Chen Y, Zhang Q, Shen T, et al. Comprehensive mutation analysis by whole-exome sequencing in 41 Chinese families with Leber congenital amaurosis. *Invest Ophthalmol Vis Sci*. 2013;54:4351–4357.
20. Waterhouse A, Bertoni M, Bienert S, et al. SWISS-MODEL: homology modelling of protein structures and complexes. *Nucleic Acids Res*. 2018;46:W296–W303.
21. Williamson KA, Hall HN, Owen LJ, et al. Recurrent heterozygous PAX6 missense variants cause severe bilateral microphthalmia via predictable effects on DNA-protein interaction. *Genet Med*. 2020;22:598–609.
22. Lee S, Lee SH, Heo H, et al. Impaired DNA-binding affinity of novel PAX6 mutations. *Sci Rep*. 2020;10:3062.
23. Hingorani M, Williamson KA, Moore AT, van Heyningen V. Detailed ophthalmologic evaluation of 43 individuals with PAX6 mutations. *Invest Ophthalmol Vis Sci*. 2009;50:2581–2590.
24. Lee B, Choi DG, Chun BY, et al. A family with a mild form of congenital nystagmus and optic disc coloboma caused by a novel PAX6 mutation. *Gene*. 2019;705:177–180.
25. Rim JH, Lee ST, Gee HY, et al. Accuracy of next-generation sequencing for molecular diagnosis in patients with infantile nystagmus syndrome. *JAMA Ophthalmol*. 2017;135:1376–1385.
26. Yahalom C, Blumenfeld A, Hendler K, et al. Mild aniridia phenotype: an under-recognized diagnosis of a severe inherited ocular disease. *Graefes Arch Clin Exp Ophthalmol*. 2018;256:2157–2164.
27. Matsushita I, Morita H, Kondo H. Autosomal dominant foveal hypoplasia without visible macular abnormalities and PAX6 mutations. *Jpn J Ophthalmol*. 2020;64:635–641.
28. Lasseaux E, Plaisant C, Michaud V, et al. Molecular characterization of a series of 990 index patients with albinism. *Pigment Cell Melanoma Res*. 2018;31:466–474.
29. Toral MA, Velez G, Boudreault K, et al. Structural modeling of a novel SLC38A8 mutation that causes foveal hypoplasia. *Mol Genet Genomic Med*. 2017;5:202–209.
30. Kuht HJ, Han J, Maconachie GDE, et al. SLC38A8 mutations result in arrested retinal development with loss of cone photoreceptor specialization. *Hum Mol Genet*. 2020;29:2989–3002.
31. Weiner C, Hecht I, Rotenstreich Y, et al. The pathogenicity of SLC38A8 in five families with foveal hypoplasia and congenital nystagmus. *Exp Eye Res*. 2020;193:107958.
32. Goolam S, Carstens N, Ross M, et al. Familial congenital cataract, coloboma, and nystagmus phenotype with variable expression caused by mutation in PAX6 in a South African family. *Molecular Vision*. 2018;24:407–413.
33. Hanson IM, Seawright A, Hardman K, et al. PAX6 mutations in aniridia. *Hum Mol Genet*. 1993;2:915–920.
34. Singh S, Stellrecht CM, Tang HK, Saunders GF. Modulation of PAX6 homeodomain function by the paired domain. *J Biological Chemistry*. 2000;275:17306–17313.
35. Lima Cunha D, Arno G, Corton M, Moosajee M. The spectrum of PAX6 mutations and genotype-phenotype correlations in the eye. *Genes*. 2019;10:1050.
36. Azuma N, Hotta Y, Tanaka H, Yamada M. Missense mutations in the PAX6 gene in aniridia. *Invest Ophthalmol Vis Sci*. 1998;39:2524–2528.
37. Yokoi T, Nishina S, Fukami M, et al. Genotype-phenotype correlation of PAX6 gene mutations in aniridia. *Hum Genome Var*. 2016;3:15052.
38. Tarilonte M, Morin M, Ramos P, et al. Parental mosaicism in PAX6 causes intra-familial variability: implications for genetic counseling of congenital aniridia and microphthalmia. *Front Genet*. 2018;9:479.
39. Landsend ES, Utheim OA, Pedersen HR, Lagali N, Baraas RC, Utheim TP. The genetics of congenital aniridia-a guide for the ophthalmologist. *Survey of Ophthalmol*. 2018;63:105–113.
40. Simpson TI, Price DJ. Pax6; a pleiotropic player in development. *Bioessays*. 2002;24:1041–1051.
41. Epstein JA, Glaser T, Cai J, Jepeal L, Walton DS, Maas RL. Two independent and interactive DNA-binding subdomains of the Pax6 paired domain are regulated by alternative splicing. *Genes Develop*. 1994;8:2022–2034.
42. Yamaguchi Y, Sawada J, Yamada M, Handa H, Azuma N. Autoregulation of Pax6 transcriptional activation by two distinct DNA-binding subdomains of the paired domain. *Genes Cells*. 1997;2:255–261.
43. Azuma N, Tadokoro K, Asaka A, et al. The Pax6 isoform bearing an alternative spliced exon promotes the development of the neural retinal structure. *Hum Mol Genet*. 2005;14:735–745.
44. Gottlob I, Proudlock FA. Aetiology of infantile nystagmus. *Curr Opin Neurol*. 2014;27:83–91.
45. Danek A. The challenge of axonal path-finding. *Strabismus*. 2006;14:95–99.
46. Huang MY, Chen CC, Huber-Reggi SP, Neuhauss SC, Straumann D. Comparison of infantile nystagmus syndrome in achiasmatic zebrafish and humans. *Ann N Y Acad Sci*. 2011;1233:285–291.
47. Harris C, Berry D. A developmental model of infantile nystagmus. *Seminars Ophthalmol*. 2006;21:63–69.

Investigative Ophthalmology & Visual Science

48. Shahzad M, Yousaf S, Waryah YM, et al. Molecular outcomes, clinical consequences, and genetic diagnosis of Oculocutaneous Albinism in Pakistani population. *Sci Rep*. 2017;7:44185.
49. You B, Zhang X, Xu K, Xie Y, Ye H, Li Y. Mutation spectrum of PAX6 and clinical findings in 95 Chinese patients with aniridia. *Molec Vis*. 2020;26:226–234.
50. Snead MP, Yates JR. Clinical and molecular genetics of Stickler syndrome. *J Med Genet*. 1999;36:353–359.
51. Papageorgiou E, McLean RJ, Gottlob I. Nystagmus in childhood. *Pediatrics and Neonatology*. 2014;55:341–351.
52. Hamming NA, Miller MT, Rabb M. Unusual variant of familial aniridia. *J Pediatric Ophthalmol Strabismus*. 1986;23:195–200.

Investigative Ophthalmology & Visual Science